Through–Bond Interactions and the Localization of Excited–State Dynamics

4 AUTHORS, INCLUDING:

Oliver Schalk
Stockholm University
34 PUBLICATIONS **234** CITATIONS

SEE PROFILE

Albert Stolow
University of Ottawa
177 PUBLICATIONS **5,145** CITATIONS

SEE PROFILE

Michael S Schuurman
National Research Council Canada
**37** PUBLICATIONS **561** CITATIONS

SEE PROFILE

Through-Bond Interactions and the Localization of Excited-State Dynamics

Oliver Schalk, Andrey E. Boguslavskiy, Albert Stolow,* and Michael S. Schuurman*

Steacie Institute for Molecular Sciences, National Research Council of Canada, 100 Sussex Dr., Ottawa, Ontario K1A 0R6, Canada

S *Supporting Information*

ABSTRACT: The influence of through-bond interactions on nonadiabatic excited-state dynamics is investigated by time-resolved photoelectron spectroscopy (TRPES) and ab initio computation. We compare the dynamics of cyclohexa-1,4-diene, which exhibits a through-bond interaction known as homoconjugation (the electronic correlation between nonconjugated double bonds), with the nonconjugated cyclohexene. Each molecule was initially excited to a 3s Rydberg state using a 200 nm femtosecond pump pulse. The TRPES spectra of these molecules display similar structure and time constants on a subpicosecond time scale. Our ab initio calculations show that similar sets of conical intersections (a [1,2]- and [1,3]-hydrogen shift, as well as carbon−carbon bond cleavage) are energetically accessible to both molecules and that the geometry and orbital composition at the minimum energy crossing points to the ground state are directly analogous. These experimental and computational results suggest that the excited-state dynamics of cyclohexa-1,4-diene become localized at a single double bond and that the effects of through-bond interaction, dominant in the absorption spectrum, are absent in the excited-state dynamics. The notion of excited-state dynamics being localized at specific sites within the nuclear framework is analogous to the localization of light absorption by a subsystem within the molecule, designated a chromophore. We propose the utility of the analogous concept, denoted here as a dynamophore.
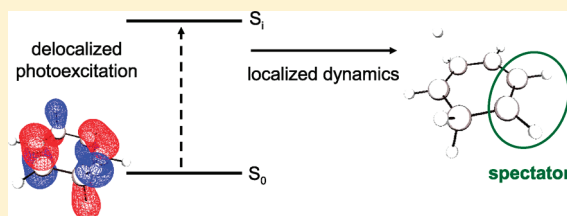
1. INTRODUCTION

The interaction of π-orbitals separated by formal isolators such as $(CH_2)_n$ groups has been widely studied[1−5] and remains an active field of research.[6−8] These interactions are classified as being either through-space or through-bond and are referred to as homoconjugation. The benchmark system for through-bond interaction is cyclohexa-1,4-diene (CHD), a planar,[9,10] cyclic molecule in which a pair of homoconjugated double bonds is separated by a single CH_2 group. The π-system of this molecule is highlighted in Figure 1. It has been stated that "the extent of interaction of two orbitals will be measured by the magnitude of the one-electron energy splitting after interaction, as compared to that splitting in the (theoretical) absence of that splitting."[1] Using this definition, the interaction of the π-orbitals is slightly larger than 1 eV in CHD,[11−14] as compared to approximately 2 eV in π-conjugated cyclohexa-1,3-diene.

While the static properties of these species have been fairly well studied, far less is known about how through-bond interactions influence molecular dynamics upon photoexcitation. The question posed here is whether photoinitiated excited-state dynamical processes become localized at one of the double bonds, or remain concerted, involving nuclear motion at both of the π-bonding sites. Specifically, is the through-bond interaction sufficiently strong so as to yield concerted dynamics, whereby the coupled electronic and nuclear wave functions are characterized by action at both double bonds?

Were the influence of homoconjugation in CHD significant, one might expect to observe dynamical processes similar to those seen in π-conjugated cyclohexa-1,3-diene. In the latter case, excitation with a UV laser pulse leads to a concerted ring-opening.[15−17] However, if the influence of homoconjugation is negligible, one would expect the dynamics of CHD to mirror that of cyclohexene (CHE), large amplitude nuclear motion about an isolated double bond. The obvious paradigm system for the latter case is the well-studied ethylene molecule. Numerous studies, both computational and experimental,[18−26] have shown that upon excitation ethylene undergoes radiationless transitions to the ground state. Recent computational work[24−27] has further demonstrated that the predominant dynamical pathways to the ground state are mediated by conical intersections. Each of the pathways initially involves torsion about the double bond, followed by pyramidalization at one of the carbon atoms. For closed-ring systems, these motions may either result in bond cleavage, hydrogen-bridge or hydrogen-transfer structures, such as the formation of an ethylidene-like species via a [1,2] H-shift. Similar dynamical processes are observed in 1,3-butadiene, torsion and pyramidalization about a carbon−carbon double bond, following from initial torsion about the central carbon single bond, which decouples the two π systems.[28]

Initial work by Wilsey and Houk provides valuable context for the present CHD and CHE study.[29,30] In those computational studies, sets of S_0−S_1 conical intersections in cyclohexene were optimized employing CASSCF methods. Low-lying intersections
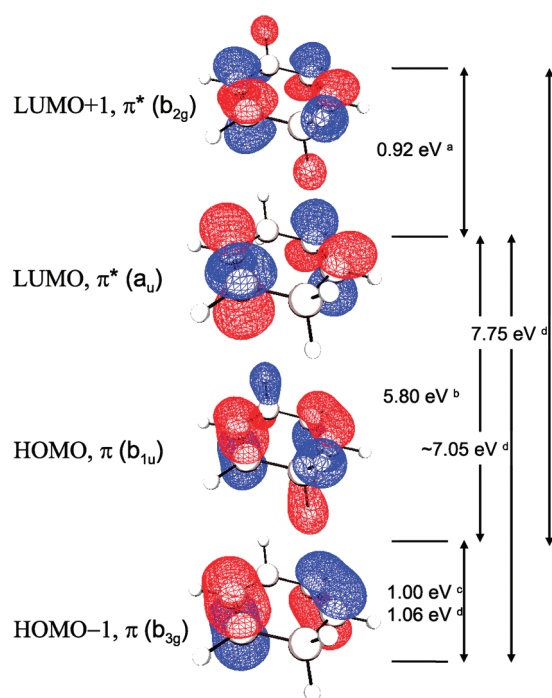
Figure 1. Orbital scheme and excitation energies for the $\pi-\pi^*$ transitions in cyclohexa-1,4-diene. Note that $a_u \leftarrow b_{1u}$ and $b_{2g} \leftarrow b_{3g}$ as well as $b_{2g} \leftarrow b_{1u}$ and $a_u \leftarrow b_{3g}$ excitations do hardly mix, although they have the same symmetry.[43] (a) Electron transmission spectroscopy, ref 57. (b) Two-photon resonance-enhanced multiphoton ionization, ref 58. (c) Photoelectron spectroscopy, refs 12,59. (d) Electron impact spectroscopy, ref 14.

were found corresponding to [1,3] hydrogen shifts, [1,2] hydrogen shifts (which corresponds to the formation of a carbene at the minimum energy crossing point), hydrogen bridged structures, and ring-opened geometries obtained from α- and β-bond cleavage. The recurrence of these ethylene-type motifs is striking and will be discussed further in the following sections.

To discuss the processes under investigation, we find it convenient to introduce the concept of a dynamophore, a direct analogue to the idea of a chromophore. A chromophore is "the part of a molecular entity in which the electronic transition responsible for a given spectral band is approximately localized."[31] Both $\pi\pi^*$ and $\pi3s$-transitions, for example, use the same chromophore: a π-orbital. Because the π-orbitals of small molecules are commonly delocalized over the whole conjugated or homoconjugated π-system, the excitation is also delocalized. By contrast, an $n\pi^*$-transition is often a localized excitation at, for example, a C=O or N—H subunit. Analogous to the concept of a chromophore, a dynamophore is the part of the molecule where the dynamics are approximately localized. While the initial response is governed by Franck—Condon active modes, the nonadiabatic transitions between electronic states often arise from a small subset of distinct molecular displacements. Furthermore, these specific displacements may be characteristic of particular bonding motifs. For the $\pi\pi^*$-excitation of cyclohexa-1,3-diene, for example, the chromophore is the conjugated double bond, while the dynamophore includes the whole carbon skeleton and spatially exceeds the chromophore.[15–17] By contrast, in butadiene, the dynamics following delocalized $\pi\pi^*$-excitation become localized at one of the C—C-double bonds,[28,32] and

thus the dynamophore is smaller than the chromophore. In this way, the dynamical response of butadiene can be understood in terms of analogous processes in ethylene. In fact, there exists the possibility of multiple distinct dynamophores being observed following a specific excitation event, depending on the topography of the potential energy surface in the Franck—Condon region.

Employing time-resolved photoelectron spectroscopy[33] (TRPES) and ab initio electronic structure methods, this study is able to show that, following initial photoexcitation, the excited-state dynamics of CHD rapidly become localized at a single double bond. The evidence for this claim comes primarily from an analysis and comparison of the similar time-resolved photoelectron spectra of CHE and CHD. This view is supported by detailed computations in which the minimum energy conical intersections, presumed to correspond to idealized funnels on the energetically accessible dynamical pathways to the ground state, are optimized for both molecules and found to be completely analogous. In addition, linearly interpolated paths from the Franck—Condon region to each intersection illuminate the evolution of excited-state energies along each path, providing a further basis for comparison between the two molecules. After a brief description of the methods in section 2, we present our results for CHD and its monoenic counterpart CHE in section 3. We compare and contrast the spectroscopic and computational data for CHD and CHE in section 4.

2. METHODS

2.1. Experiment. Cyclohexa-1,4-diene and cyclohexene were obtained from Sigma-Aldrich and Alfa-Aesar, respectively, with nominal purities of 99%. Both samples were used without further purification.

Time-resolved photoelectron spectra were recorded in a magnetic bottle apparatus, described in detail elsewhere.[34,35] A supersonic molecular beam of seed gas in 3 bar of helium was expanded into vacuum using an Even-Lavie valve (250 μm nozzle diameter) at a repetition rate of 1 kHz. A Ti:sapphire regenerative amplifier (Coherent, Legend Elite) pumped by two 1 kHz Nd:YLF lasers (Coherent, Evolution) was seeded by a Ti:sapphire oscillator (Spectra Physics, Tsunami), itself pumped by a Nd:YLF diode pumped laser (Spectra Physics, Millennia). Harmonics were generated by doubling the fundamental beam and subsequent sum frequency generation in BBO-crystals. Pump energies were of 500 nJ/pulse for the 200 nm pump pulse and 2 μJ/pulse for the 267 nm probe pulse. The pulses were weakly focused into the interaction region by $f/100$ spherical reflective optics, and the polarization states of the laser pulses were individually controlled by Berek compensators (New Focus) and set to magic angle with respect to each other. The in situ cross-correlation was measured to be τ_{cc} = 130 fs. The time delay between the two pulses was controlled by using a motorized linear translation stage. At each time delay, the measured pump—probe signal was corrected by dynamically subtracting background signals due to pump and probe pulses alone.

2.2. Computational Details. The minimum energy S_0-S_1 conical intersections were determined employing ab initio electronic structure methods, as were the paths from the C_2 and D_{2h} symmetry ground-state minimum energy geometries of CHE and CHD, respectively, to sets of minimum energy conical intersections (MECI) determined via the linear interpolation of the internal coordinates.

The optimized geometries for points on the CHE and CHD potential energy surfaces were obtained from multireference configuration interaction wave functions, limited to double excitations (MR-CISD) based on complete active space self-consistent field (CASSCF) references and employing the 3s2p1d and 2s1p atomic natural orbital (ANO) basis sets

for C and H, respectively.[36,37] The various MECIs between the S_0 and S_1 electronic states, discussed below, were energy minimized employing active spaces comprised of the π orbitals and averaging over the lowest 3 (6) states of CHE (CHD). Dynamic correlation was included at the MR-CISD level of theory. These geometry optimizations included the valence states only. All MRCI computations were performed using the COLUMBUS suite of programs.[38,39]

To determine the valence and 3s Rydberg electronic energies along the paths, a 3s Rydberg orbital was generated using MOLCAS[37,40] and, employing optimized cationic orbitals, expanded in a set of universal exponents.[41] For points along the path, the center of the Rydberg basis was located at the center of mass of the carbon atoms, thereby approximating the center of charge of the molecule. This approximation is quite reasonable for points near the Franck–Condon region, where an accurate determination of the Rydberg state energies is most important. The vertical excitation energies were computed at the Davidson-corrected MR-CISD level of theory. The ionization potentials, relative to the ground-state minimum, were also determined for each point along the interpolated paths at the same level of theory. These latter data are presented as Supporting Information.

3. RESULTS

3.1. Ab Initio Computations. We begin by summarizing the computational results for these systems to provide context for the discussion of the time-resolved photoelectron spectra presented in the following section.

3.1.1. Franck–Condon Region. A straightforward, if incomplete, evaluation of the computational methods used in this study can be made employing the vertical excitation energies. To this end, the computed energy of the π3s state of CHE at 6.39 eV is in reasonable agreement with the spectroscopically determined value of 5.92 eV.[42] While the 7.76 eV excitation energy to the $\pi\pi^*$ is somewhat higher than the absorption maximum near 6.89 eV, it is consistent with the large geometric relaxation expected on the excited state. The bright $\pi\pi^*$ state ($I = 0.658$) will clearly have the largest oscillator strength, I, from the ground state for one photon absorption processes, but the significantly weaker 3s transition ($I = 0.028$) is also symmetry allowed.

The vertical excitation energies for CHD have been rigorously determined by Roos and co-workers employing CASPT2 computations and ANO basis sets.[43] These calculations, which are in good agreement with electron impact spectra,[14] predict the first and second excited states to be the valence $\pi\pi^*$ $^1B_{1g}$ and 3s Rydberg $^1B_{1u}$ states, respectively. The $\pi\pi^*$ state is optically dark for one-photon processes, whereas the $\pi \longrightarrow$ 3s Rydberg state is weakly absorbing. The corresponding MRCI $\pi\pi^*$ and lowest π3s excitation energies, computed here to be 6.58 and 6.12 eV, respectively, are somewhat larger than the previous computational (5.74 eV, 5.90 eV) and experimental (5.80 eV, 6.10 eV) results, particularly the energy of the lowest $\pi\pi^*$ state. As all of these results show, the energy gap between the lowest Rydberg and valence states is quite small, and, in fact, the current computations invert the ordering of lowest $\pi\pi^*$ and π3s states in the Franck–Condon region. This feature of the CHD interpolated paths, while important to note, does not significantly impact the conclusions that can be drawn from these computations.

3.1.2. Dynamical Pathways. In agreement with previous studies by Houk and Wilsey,[29,30] we have found that the low-lying conical intersections in CHE and CHD may be grouped into four classes. These are described as a [1,2] hydrogen bridge,
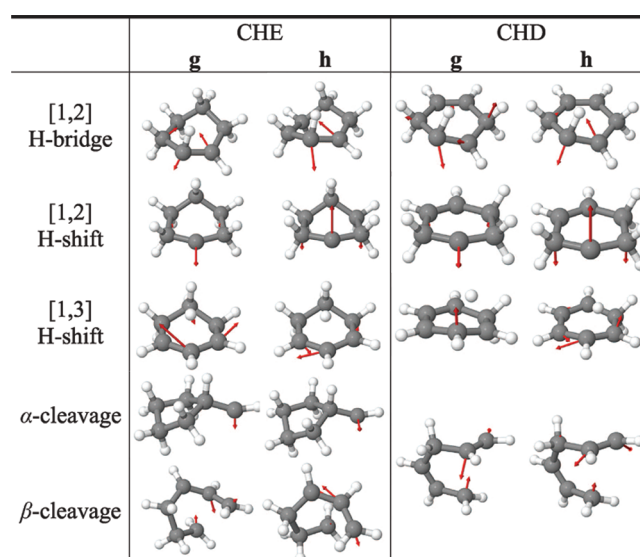

Figure 2. Branching space vectors for S_0/S_1 intersections of CHE and CHD. The rows denote the minimum energy crossing points corresponding to the [1,2] H-bridge, [1,2] H-shift, [1,3] H-shift, α-bond cleavage, and β-bond cleavage intersections, respectively.

a [1,2] hydrogen shift, a [1,3] hydrogen shift, and (α- or β-) bond cleavage. The intersection geometries are shown pictorially in Figure 2, while the tabular Cartesian geometries are provided in the Supporting Information. In addition to the optimized structures, the corresponding **g** and **h** vectors[44] are also shown. These vectors, determined by the energy difference gradient between the two intersecting states (**g**-direction) and the non-adiabatic coupling gradient (**h**-direction), define the coordinates, which lift the degeneracy linearly as one moves away from the conical intersection and together define the branching space.[45] It is movement along the directions in this space that is predicted to be particularly efficient at "routing"[46] wavepackets from one electronic state to another.

These MECI serve as the end point for each of the interpolated paths shown in Figure 3. While the interpolated paths may be a rough approximation to the actual evolution of the vibronic wavepacket because they neglect the initial dynamics governed by Franck–Condon active modes, they are useful insofar as they show the relative change in the low-lying electronic states along the progress coordinate, as well as give some indication about potential barriers between the Franck–Condon and crossing regions. These paths show that the behavior of the low-lying excited states is quite similar in both CHE and CHD. In both CHE paths, the lowest $\pi\pi^*$ state (red) crosses with the 3s Rydberg state (green) relatively near the Franck–Condon point. However, as stated above, the present level of ab initio calculations reverses the energetic ordering of the 3s and lowest $\pi\pi^*$ in CHD, yielding interpolated paths nearly identical to those of CHE. Rather, the small energy separation between the dark $\pi\pi^*$ and 3s state will certainly engender rapid, intersection-mediated internal conversion between the states. The large gradients on the valence manifold then direct the vibronic wavepacket to one of the MECIs discussed below.

The instantaneous vertical ionization potentials, computed relative to the ground-state minimum, generally increase upon dynamical evolution from approximately 8.5 to 11 eV for CHE and 9 to 11 eV for CHD, consistent with the experimental results.
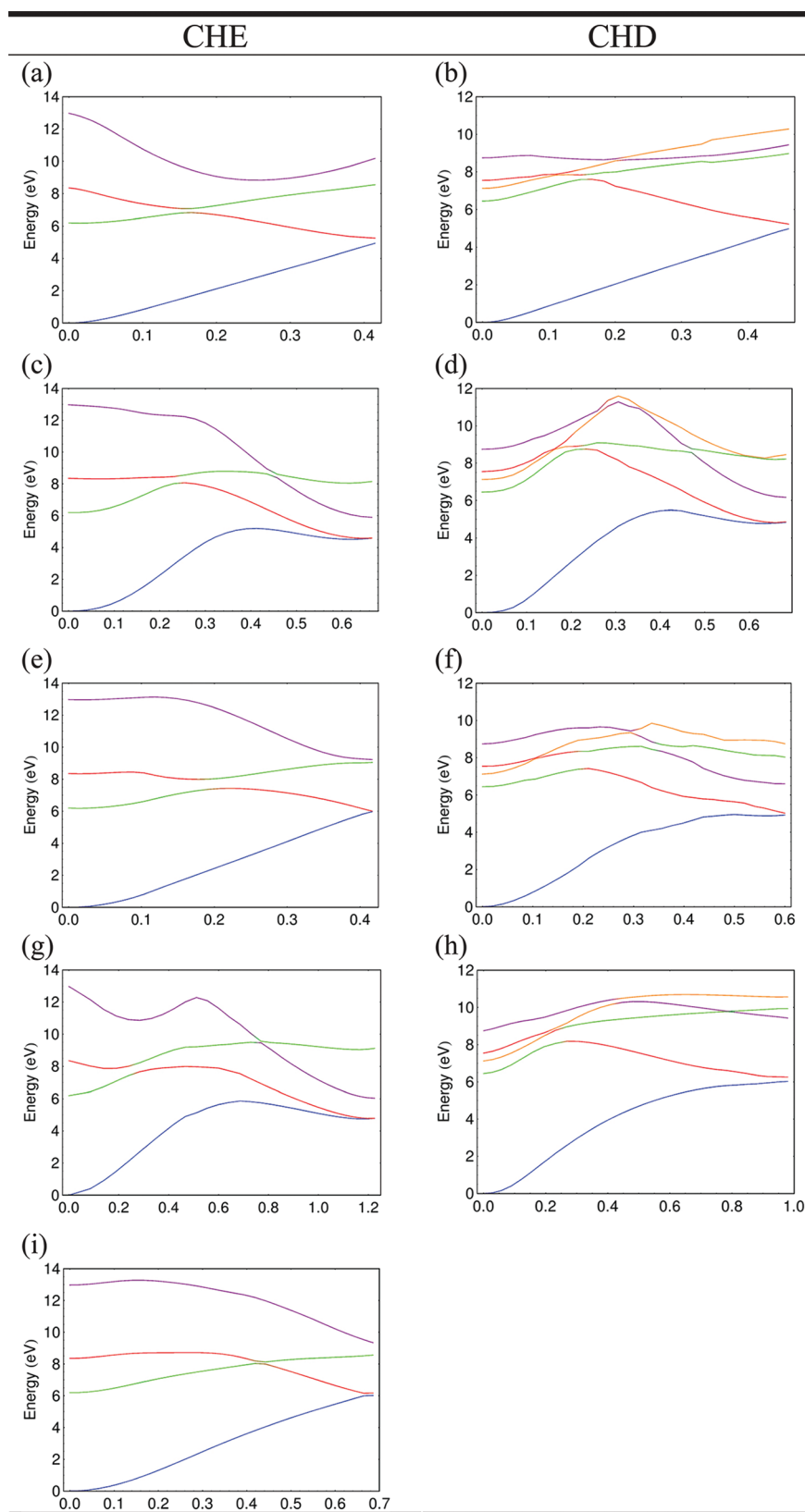
Figure 3. Electronic state energies along linearly interpolated paths with displacement coordinate x, corresponding to the distinct S_0/S_1 conical intersections of CHE and CHD. The coloring of the lines conveys the electronic character of the states, such that blue, green, red (and orange for CHD), and purple lines correspond to the ground, $\pi 3s$, $\pi\pi^*$, and $(\pi^*)^2$ states respectively. Panels (a) and (b), (c) and (d), (e) and (f), and (g), (h), and (i) correspond to the $[1,2]$ H-bridge, $[1,2]$ H-shift, $[1,3]$ H-shift, and bond cleavage intersections in CHE and CHD, respectively. The mass-weighted reaction coordinate is in units of Å amu$^{-1/2}$.
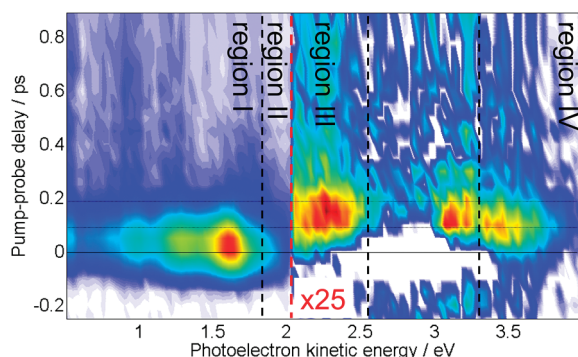
Figure 4. TRPES spectrum of cyclohexene at a pump wavelength of $\lambda_p = 200$ nm and a probe wavelength of $\lambda_e = 267$ nm. Regions III and IV are multiplied by a factor of 25. In these regions, two probe photons are required for ionization.
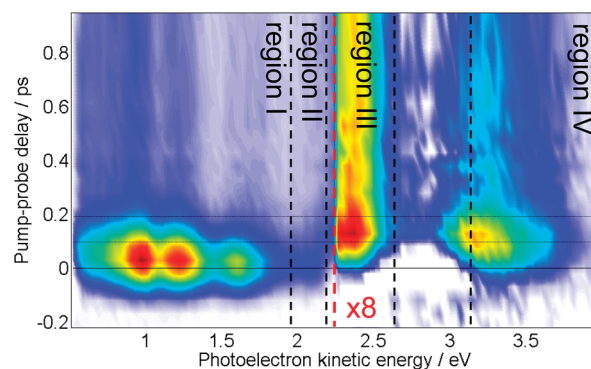

Figure 5. TRPES spectrum of cyclohexa-1,4-diene at a pump wavelength of $\lambda_p = 200$ nm and a probe wavelength of $\lambda_e = 267$ nm. Regions III and IV are multiplied by a factor of 8. In these regions, two probe photons are required for ionization.

3.1.3. Hydrogen Shifts. The [1,2] H-shift gives rise to an $S_0 - S_1$ intersection in which a singlet carbene is formed at one of the carbons formerly involved in the double bond. The **g**- and **h**-directions for CHE and CHD are practically identical (see Figure 2), with the **g**-direction associated with an in-plane C−C−C angle bend, while the **h**-direction is described by the out-of-plane wagging mode of the carbene carbon atom. The directions that define the branching space for intersections involving a hydrogen bridge across the double bond are presented in Figure 2b. While the **g**- and **h**-directions for CHE and CHD are completely analogous, they are quite different from the [1,2] H-shift vectors. Upon closer inspection, it is clear that [1,2] H-shift and [1,2] H-bridge intersections are analogous to the [1,2] H-shift and [1,2] H-bridge intersection in ethylene,[26] further evidence that both of these molecules would be expected to undergo similar excited-state dynamical processes.

The $S_1 - S_0$ intersections involving a [1,3] H-shift differ from the [1,2] case in that the minimum energy crossing point is very similar to the transition state for the Woodward−Hoffmann forbidden ground-state hydrogen shift reaction, and, moreover, it constitutes a sigmatropic rearrangement. As Figure 2 shows, the migrating hydrogen atom is located directly above the 2-carbon. As for the [1,3] H-shift, the **g**- and **h**-vectors are almost identical and show a C−C-stretch along one of the former π-bonds.

An examination of the molecular orbitals (given pictorially as Supporting Information) shows that for each conical intersection type, the CHD molecular orbitals evidence two distinct π-systems, in which one of the bonding/antibonding π-orbital pairs is left largely unperturbed. This behavior suggests that the CHD dynamophores do not include the homoconjugated double bond in any of the relevant processes. Additionally, the contours of the linear interpolations in Figure 3a and b demonstrate that a dynamical treatment of this system would necessarily include a description of the doubly excited $(\pi^*)^2$ state (purple), which drops precipitously in energy to lie only 1 eV above the $S_0 - S_1$ conical intersection. This state correlates to the dark Z-state discussed in previous studies.[29,30,47]

3.1.4. Ring-Opening and Contraction. Focusing now on those $S_1 - S_0$ intersections involving the ring-opening cleavage of a carbon−carbon single bond, CHE displays crossings that correspond to both an α- and a β-cleavage of carbon−carbon single bonds, while CHD has one unique carbon−carbon single bond that can be broken. All three intersections are qualitatively similar. Their **g** vectors point toward ring-closure, which likely

Table 1. Time Constants for the Dynamics of Cyclohexene and Cyclohexa-1,4-diene Extracted from Global Fits to the TRPES Data[a]

region	electron KE/eV	delay/fs	time constants
		Cyclohexene	
I	0.6−1.6	20−50[b]	$\tau_2^{CHE} = 30 \pm 10$ fs
			$\tau_5^{CHE} = 0.5-2$ ps[c]
II	1.8−2.0	0	$\tau_1^{CHE} = 40 \pm 10$ fs
			$\tau_5^{CHE} = 500$ fs
III	2.0−2.35	90	$\tau_3^{CHE} = 175 \pm 50$ fs
			$\tau_6^{CHE} = 5 \pm 1.5$ ps
IV	3.35−3.85	90	$\tau_4^{CHE} = 60 \pm 15$ fs
			$\tau_6^{CHE} = 5 \pm 1.5$ ps
		Cyclohexa-1,4-diene	
I	0.6−1.8	20−80[b]	$\tau_2^{CHD} = 50 \pm 10$ fs
			$\tau_5^{CHD} = 1.3 \pm 0.3$ ps
II	1.86−2.1	20	$\tau_{1+2}^{CHD} = 65 \pm 15$ fs
			$\tau_5^{CHD} = 1.3 \pm 0.3$ ps
III	2.2−2.6	100	$\tau_3^{CHD} = 60 \pm 10$ fs
			$\tau_6^{CHD} = 1.6 \pm 0.3$ ps
IV	3.35−3.85	100	$\tau_3^{CHD} = 60 \pm 10$ fs
			$\tau_6^{CHD} = 1.6 \pm 0.3$ ps

[a] The different regions are defined in Figures 4 and 5; the numbering relates to the time-ordering of the observed processes. The delay refers to an artificial shift of time zero as explained in the Supporting Information. Not listed are the time constants for the additional rise on the picosecond-time scale. See section 3 for the assignment of the time constants and further discussion. [b] Continuous shift of time zero due to severe deformations of the molecule. [c] The decay time changes throughout the spectrum, indicating a deformation of the molecule, which is typical for ground-state rearrangements.

occurs as consecutive dynamics in the ground state, and is discussed in more detail in the Supporting Information. In fact, the α-cleavage MECIs appear to have already undergone ring
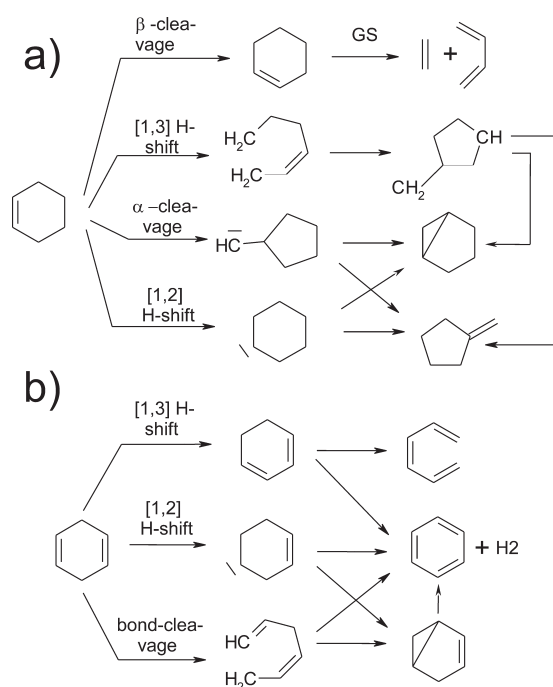
Figure 6. Reaction paths for (a) cyclohexene and (b) cyclohexadiene upon photoexcitation. The first step shows the initial rearrangement due to the excitation; the following steps are possible consecutive reactions in the hot ground state. For details, see refs 47,50 and the Supporting Information.

closure. In agreement with the other MECIs discussed above, the homoconjugated double bond in CHD is again left unperturbed, as the orbitals along the interpolated pathways indicate (see the Supporting Information).

3.2. Time-Resolved Photoelectron Spectra. Time-resolved photoelectron spectra of CHE and CHD at a pump wavelength of $\lambda_p = 200$ nm (6.2 eV) and a probe wavelength of $\lambda_e = 267$ nm (4.65 eV) are shown in Figures 4 and 5, respectively. Because both molecules are mainly excited to the $\pi 3s$-Rydberg state when pumped at 200 nm (see discussion on the apparently delayed rise of CHD in the Supporting Information), subsequent evolution on related potential energy surfaces allows for a direct comparison of the two spectra. Given the range of energetically accessible pathways implied by the theoretical studies of Wilsey and Houk,[29,30] as well as our computational results, it is not surprising that the measured TRPES shows a myriad of spectral features.

Time constants characterizing the evolution of the photoelectron spectra were determined by a Levenberg—Marquart global fitting routine, as described in ref 48. A short summary of the method as well as a detailed analysis of the fitting procedure are given in the Supporting Information, while the extracted time constants are given in Table 1. Here, we highlight the main features of the spectra necessary to discuss the influence of homoconjugation on the excited-state dynamics in CHD. In Figure 6, we present a reaction scheme highlighting the initial processes and potential consecutive reactions. Because we did not study ground-state processes explicitly, the reader is referred to refs 47 and 50 for more details on these reactions in CHE and CHD, respectively.

As seen in Figures 4 and 5, both TRPES spectra have similar structure. This is evidenced in the figures by the segmentation of

the spectra into different photoelectron kinetic energy regimes wherein both molecules exhibit analogous spectral features. We find that the following mechanism can be applied to both CHE and CHD and is consistent with both the experimental and the computational findings.

Upon initial excitation to the $\pi 3s$-Rydberg state, nuclear dynamics on this potential energy surface are observed in region II. The photoelectron signal rises at time zero and is depopulated within τ_1 to a lower lying state seen in region I of the TRPES spectrum. This lower state is most likely the lowest lying $\pi\pi^*$ state, as suggested by the computational results. The rise of the signal in region I is delayed by $\sim\tau_1$, which is a strong indication that these dynamics follow sequentially from region II.

In region I, the time shift of the photoelectron signal corresponding to ionization of the $\pi\pi^*$-state to the ionic ground state could arise from: (a) large amplitude motion, for example, in the ring-opening channels, thereby changing the Franck—Condon overlap between the initial and final state, (b) a significant change in the character in the wave function yielding a different set of electronic correlations in the ionic continuum, and/or (c) an increase in the ionization potential engendered by a rapid decrease in the electronic energy of the excited state due to vibrational dynamics.

The signals observed in regions III and IV are further delayed in time and originate from two-probe photon ionization of the excited state. One possible origin of this signal is the $(\pi^*)^2$ state; however, our calculations have shown that this state likely does not take part in the reaction process (see section 3.1.2 and Figure 3, although questions concerning the involvement of this state will be more definitively answered by trajectory calculations). This result is consistent with what might be expected from an ethylenic model, where the $\pi\pi^*$ and the $(\pi^*)^2$ states are degenerate at high symmetry geometries corresponding to a 90° twist about the C—C-bond. In the present case, the twisting angle is significantly less than 90°, leaving the $(\pi^*)^2$ state almost 1 eV higher in energy at the MECI. We suggest that the signal in these regions might also originate from the $\pi\pi^*$ state. As the computations predict, the instantaneous vertical ionization potentials of the molecules rise above the 1+1 threshold at 10.85 eV when the dynamics approaches the conical intersections (see plots in the Supporting Information). Hence, two photons are necessary for ionization. The different femtosecond-time constants seen in regions I, III, and IV might indicate different reaction channels, while the longtime behavior can be assigned to "hot" ground-state dynamics. These are discussed in the Supporting Information.

The spectral data and extracted time constants from previous femtosecond-ion yield studies of CHE and CHD[47,49—51] generally agree with the present data. However, TRPES permits more definitive conclusions to be drawn about the excited-state dynamics of these molecules. In particular, we can exclude a 10 fs return to the ground state as was claimed in ref 49. Fuss et al. inferred the presence of the $(\pi^*)^2$ state in the dynamical pathway from the appearance of a highly fragmented species in their strong field ionization probe experiments.[47] Unfortunately, from our TRPES results, we cannot make inferences about the participation of the $(\pi^*)^2$ state in the dynamics. We note, however, that polyatomic molecules in strong laser fields can exhibit very complex ionization—fragmentation dynamics,[52] and it may be difficult to unambiguously assign a fragmentation channel to a specific electronic character.

4. DISCUSSION

4.1. Localization of Dynamics. On the basis of our TRPES studies and ab initio computations, we suggest that the effect of through-bond interaction on excited-state dynamics is marginal and that a single mechanism in which large amplitude nuclear motion becomes localized at a single double bond can be applied to both the CHE and CHD molecular species. In the TRPES experiments, both molecules were excited to the same electronic potential energy surface, the lowest lying $\pi 3s$-Rydberg state. The difference between the two excitation processes is that the chromophore is localized at the double bond in CHE but delocalized over the homoconjugated double bonds in CHD. Nevertheless, both molecules show very similar dynamics, and their spectra exhibit similar features (see Figures 4 and 5), enabling us to model both employing the same kinetic mechanism (section 3.2). Although the time constants and the long time behavior are different, the general spectral features indicate that the same dynamophore is at work in both molecules. These differences are not surprising given the difference in the relative energies between the low-lying valence states and the initially populated 3s Rydberg state of CHE and CHD. The long time behavior can be rationalized by different ground-state channels, as is further discussed in the Supporting Information (see also Figure 6).

In addition to the experimental data, our ab initio calculations corroborate the hypothesis of strongly localized dynamics in CHD. Specifically, given that the interpolated paths of CHE and CHD are very similar, and that one pair of π and π^* orbitals along the interpolated paths of CHD persist as only slightly perturbed spectators, and that the respective MECIs display analogous geometrical structures and branching spaces, our results strongly suggest that both molecules exhibit similar dynamical behavior following photoexcitation. Almost all of the intersection types determined here have direct analogues to the seams of intersection observed in ethylene. The [1,2] H-shift and [1,2] H-bridge intersections in CHE and CHD correspond to the previously discussed ethylidene-like and H-bridged intersections, respectively.[21,22,25,26,53] Likewise, in closed-ring systems, twisted-pyramidalized geometries may involve the breaking of the adjacent C–C bonds, as seen in the α- and β-cleavage processes for CHE and the single-bond breaking path in CHD. Obviously, there is no clear analogue to the [1,3] H-migration pathway observed in ethylene; however, the efficacy of this intersection type is likely highly dependent both on the twist-pyramidalization displacements required to promote hydrogen bond cleavage and migration, as well as on the ring structure that provides an initial conformationally locked geometry. That the dynamical processes observed in ethylene find such a clear correlation with the observed processes not only in CHE, but also in CHD, provides further evidence that the effect of through-bond interaction on the excited-state dynamics of CHD is minimal. The dynamophore in CHD appears to be a lone C=C-bond or, to be more precise, the CH=CH–CH$_2$-moiety.

4.2. Impetus To Localize Dynamics. To this point, we have presented evidence for the localization of dynamics in CHD following delocalized photoexcitation. However, a more fundamental question is: what is the origin of this behavior? In the case of butadiene, the process that decouples the strongly interacting π systems is large amplitude rotation about the C–C single bond. By contrast, in CHD, the ring system cannot be decoupled in the same way because this internal rotation is constrained.

However, if the magnitude of the π-interaction is very small, one might equally expect a localization of the dynamical process following only small deformations. The effect of through-bond interactions is strongly evident in static absorption spectroscopy, for example, by comparing the static photoelectron spectra of CHE and CHD. The first ionic state of CHE is a single band, while the analogous transition splits into two bands in CHD[12] (other studies referring to orbital energies are cited in Figure 1). Therefore, the question arises as to why this apparently strong interaction has such a minor impact on the excited-state dynamics.

At the highly symmetric Franck–Condon geometry, the electronic overlap between the π orbitals on the ethylenic moieties is mediated by C–H σ-bond on the bridging carbons (see Figure 1). Because of their p-orbital like structure, we imagine that this through-bond coupling will be highly sensitive to angular misalignment. At the Franck–Condon point, the through-bond interaction leads to in-phase and out-of-phase combinations of the π-systems and the observed splitting in the absorption and photoelectron spectra. For dynamics to become localized, we require interactions that will couple these in-phase and out-of-phase electronic wave functions, leading to localization on one C=C-bond only. Because of the anticipated strong dependence of the through-bond coupling on the angular displacement of the C–H σ-orbitals, we imagine that very small distortions will rapidly reduce the splitting between the in-phase and out-of-phase wave functions to the extent that they approach near degeneracy at distorted geometries. At this point, another molecular vibration can nonadiabatically mix these two states, leading to a localization of excitation on a single C=C-bond alone. Once dynamical localization occurs, rapid "ethylenic dynamics" (i.e., torsion) at a single C=C bond leads to apparently irreversible behavior and the emergence of a single CH$_2$–CH=CH as a main dynamophore in the excited-state photochemistry of CHD.

5. CONCLUSION

In the present investigation, we showed both experimentally and theoretically that the influence of through-bond interaction on excited-state dynamics in the model system cyclohexa-1,4-diene is marginal. Rather, the dynamical processes become localized about one of the double bonds, leading to TRPES results that are qualitatively the same as those observed for cyclohexene. Thus, the additional π-system acts dynamically as a spectator, a behavior that has been found in other, albeit less geometrically constrained, conjugated species such as butadiene.[28,32] Localization occurs via the symmetry lowering of the nuclear framework, a process engendered by molecular vibrations and gradients of the excited-state potential energy surface, thereby decoupling the interacting ethylenic moieties. While these forces may be insufficient to surmount the π-conjugation observed in cyclohexa-1,3-diene, the weaker through-bond interaction, with its particular sensitivity to internal angular displacements, is easily overcome.

The recurrence of ethylenic-type dynamical processes in a number of larger unsaturated hydrocarbons suggests that photoexcitation of molecules with π-bonds can perhaps be understood in terms of local chemical moieties, dynamophores, within the molecular framework. This notion is common within aromatic systems, for example, when functional groups are attached to a benzene ring where the whole molecule acts as a chromophore

but the dynamics mainly take place at the functional groups (e.g., stilbene[53−55] or substituted paracyclophanes[56]). We emphasize that the realization that even small polyenes tend to localize their dynamics is relatively new. The more general utility of the concept of a dynamophore will be further evaluated in subsequent reports.

■ ASSOCIATED CONTENT

Ⓢ   **Supporting Information.**   Fitting procedure, in depth analysis of the data, ground-state processes, ionization potentials for the interpolated paths, orbitals and geometries of the ground state, and the MECIs for CHE and CHD. This material is available free of charge via the Internet at http://pubs.acs.org.

■ AUTHOR INFORMATION

Corresponding Author
albert.stolow@nrc.ca; michael.schuurman@nrc.ca

■ ACKNOWLEDGMENT

■ REFERENCES

(1) Hoffmann, R. *Acc. Chem. Res.* **1971**, *4*, 1.
(2) Gleiter, R. *Angew. Chem., Int. Ed. Engl.* **1974**, *13*, 696.
(3) Paddon-Row, M. N. *Acc. Chem. Res.* **1982**, *15*, 245.
(4) Martin, H.-D.; Mayer, B. *Angew. Chem., Int. Ed. Engl.* **1983**, *22*, 283.
(5) Gleiter, R.; Schaefer, W. *Acc. Chem. Res.* **1990**, *23*, 369.
(6) Lovitt, C. F.; Dong, H.; Hrovat, D. A.; Gleiter, R.; Borden, W. T. *J. Am. Chem. Soc.* **2010**, *132*, 14617.
(7) Wei, H.; Hrovat, D. A.; Mo, Y.; Hoffmann, R.; Borden, W. T. *J. Phys. Chem. A* **2009**, *113*, 10351.
(8) Palusiak, M.; Krygowski, T. M. *Chem. Phys. Lett.* **2009**, *481*, 34.
(9) Rabideau, P. W. *Acc. Chem. Res.* **1978**, *11*, 141.
(10) Lipkowitz, K. B.; Rabideau, P. W.; Raber, D. J.; Hardee, L. E.; Schleyer, P. v. R.; Kos, A. J.; Kahn, R. A. *J. Org. Chem.* **1982**, *47*, 1002.
(11) Kishimoto, N.; Ogasawara, H.; Ohno, K. *Bull. Chem. Soc. Jpn.* **2002**, *75*, 1503.
(12) Bischof, P.; Hashmall, J. A.; Heilbronner, E.; Hornung, V. *Helv. Chim. Acta* **1969**, *52*, 1745.
(13) Frueholz, R. P.; Flicker, W. M.; Mosher, O. A.; Kuppermann, A. *J. Chem. Phys.* **1979**, *70*, 1986.
(14) McDiarmid, R.; Doering, J. P. *J. Chem. Phys.* **1981**, *75*, 2687.
(15) Kosma, K.; Trushin, S. A.; Fuss, W.; Schmid, W. E. *Phys. Chem. Chem. Phys.* **2009**, *11*, 172.
(16) Dou, Y.; Yuan, S.; Lo, G. V. *Appl. Surf. Sci.* **2007**, *253*, 6404.
(17) Tamura, H.; Nanbu, S.; Ishida, T.; Nakamura, H. *J. Chem. Phys.* **2006**, *124*, 084313/1.
(18) Collin, G. J.; Deslauriers, H.; Makulski, W. *J. Photochem.* **1987**, *39*, 1.
(19) Stolow, A.; Balko, B. A.; Cromwell, E. F.; Zhang, J. S.; Lee, Y. T. *J. Photochem. Photobiol.* **1992**, *62*, 285.
(20) Farmanara, P.; Stert, V.; Radloff, W. *Chem. Phys. Lett.* **1998**, *288*, 518.
(21) Kosma, K.; Trushin, S. A.; Fuss, W.; Schmid, W. E. *J. Phys. Chem. A* **2008**, *112*, 7514.
(22) Barbatti, M.; Paier, J.; Lischka, H. *J. Chem. Phys.* **2004**, *121*, 11614.
(23) Ben-Nun, M.; Martinez, T. J. *Chem. Phys. Lett.* **1998**, *57*, 298.
(24) Ben-Nun, M.; Quenneville, J.; Martinez, T. J. *J. Phys. Chem.* **2000**, *104A*, 5161.
(25) Barbatti, M.; Ruckenbauer, M.; Lischka, H. *J. Chem. Phys.* **2005**, *122*, 174307.

(26) Tao, H.; Levine, B. G.; Martinez, T. J. *J. Phys. Chem. A* **2009**, *113*, 13656.
(27) Barbatti, M.; Granucci, G.; Persico, M.; Lischka, H. *Chem. Phys. Lett.* **2005**, *401*, 276.
(28) Levine, B. G.; Martinez, T. J. *J. Phys. Chem. A* **2009**, *113*, 12815.
(29) Wilsey, S.; Houk, K. N. *J. Am. Chem. Soc.* **2000**, *122*, 2651.
(30) Wilsey, S.; Houk, K. N. *J. Am. Chem. Soc.* **2002**, *124*, 11182.
(31) IUPAC. *Compendium of Chemical Terminology*, 2nd ed.; doi: 10.1351/goldbook.C01076.
(32) Wilsey, S.; Houk, K. N. *Photochem. Photobiol.* **2002**, *76*, 616.
(33) Stolow, A.; Underwood, J. G. *Adv. Chem. Phys.* **2008**, *139*, 497.
(34) Kruit, P.; Read, F. H. *J. Phys. E* **1983**, *16*, 313.
(35) Lochbrunner, S.; Larsen, J. J.; Shaffer, J. P.; Schmitt, M.; Schulz, T.; Underwood, J. G.; Stolow, A. *J. Electron Spectrosc. Relat. Phenom.* **2000**, *112*, 183.
(36) Pierloot, K.; Dumez, B.; Widmark, P.-O.; Roos, B. O. *Theor. Chim. Acta* **1995**, *90*, 87.
(37) Roos, B. O.; Andersson, K.; Fulscher, M. P.; Malmqvist, P.-A.; Serrano-Andres, L. *Adv. Chem. Phys.* **1996**, *63*, 219.
(38) Shepard, R.; Shavitt, I.; Pitzer, R. M.; Comeau, D. C.; Pepper, M.; Lischka, H.; Szalay, P. G.; Ahlrichs, R.; Brown, F. B.; Zhao, J. *Int. J. Quantum Chem., Quantum Chem. Symp.* **1988**, *22*, 149.
(39) Lischka, H.; Shepard, R.; Shavitt, I.; Pitzer, R. M.; Dallos, M.; Mueller, T.; Szalay, P. G.; Seth, M.; Kedziora, G. S.; Yabushita, S.; Zhang, Z. *Phys. Chem. Chem. Phys.* **2001**, *3*, 664.
(40) Karlstrom, G.; Lindh, R.; Malmqvist, P. A.; Roos, B. O.; Ryde, U.; Veryazov, V.; Widmark, P. O.; Cossi, M.; Schimmelpfennig, B.; Neogrady, P.; Seijo, L. *Comput. Mater. Sci.* **2003**, *28*, 222.
(41) Kaufmann, K.; Baumeister, W.; Jungen, M. *J. Phys. B: At. Mol. Opt. Phys.* **1989**, *22*, 2223.
(42) Watson, H. F., Jr.; McGlynn, S. P. *Theor. Chim. Acta* **1971**, *21*, 309.
(43) Merchan, M.; Serrani-Andres, L.; Slater, L. S.; Roos, B. O.; McDiarmid, R.; Xing, X. *J. Phys. Chem. A* **1999**, *103*, 5468.
(44) Yarkony, D. R. *Acc. Chem. Res.* **1998**, *31*, 511.
(45) Atchity, G. J.; Xantheas, S. S.; Ruedenberg, K. *J. Chem. Phys.* **1991**, *95*, 1862.
(46) Yarkony, D. R. *J. Chem. Phys.* **2001**, *114*, 2601.
(47) Fuß, W.; Schmid, W. E.; Trushin, S. A. *J. Am. Chem. Soc.* **2001**, *123*, 7101.
(48) Schalk, O.; Boguslavskiy, A. E.; Stolow, A. *J. Phys. Chem. A* **2010**, *114*, 4058.
(49) Diau, E. W.-G.; Feyter, S. D.; Zewail, A. H. *J. Chem. Phys.* **1999**, *110*, 9785.
(50) Feyter, S. D.; Diau, E. W.-G.; Zewail, A. H. *Phys. Chem. Chem. Phys.* **2000**, *2*, 877.
(51) Mestdagh, J. M.; Visticot, J. P.; Elhanine, M.; Soep, B. *J. Chem. Phys.* **2000**, *113*, 237.
(52) Lezius, M.; Blanchet, V.; Ivanov, M. Y.; Stolow, A. *J. Chem. Phys.* **2002**, *117*, 1575.
(53) Martinez, T. J. *Acc. Chem. Res.* **2006**, *39*, 119.
(54) Dou, Y.; Wu, W.; Tang, H.; Allen, E. *Chem. Phys.* **2008**, *353*, 104.
(55) Takeuchi, S.; Ruhman, S.; Tsuneda, T.; Chiba, M.; Takesugu, T.; Tahara, T. *Science* **2009**, *322*, 1073.
(56) Brogaard, R. Y.; Boguslavskiy, A. E.; Schalk, O.; Enright, G. D.; Hopf, H.; Raev, V.; Jones, P. G.; Thomsen, D. L.; Solling, T. I.; Stolow, A. *Chem.-Eur. J.* **2011**, *17*, 3922.
(57) Jordan, K. D.; Michejda, J. A.; Burrow, P. D. *Chem. Phys. Lett.* **1976**, *42*, 227.
(58) Roos, B. O.; Merchan, M.; McDiarmid, R.; Xing, X. *J. Am. Chem. Soc.* **1994**, *16*, 5927.
(59) Bieri, G.; Burger, F.; Heilbronner, E.; Meier, J. P. *Helv. Chim. Acta* **1977**, *60*, 2213.